6856 *Biochemistry* **2010,** *49,* 6856–6865
DOI: 10.1021/bi100857g

BIOCHEMISTRY
including biophysical chemistry & molecular biology
*Article*

# Polar Groups in Membrane Channels: Consequences of Replacing Alanines with Serines in Membrane-Spanning Gramicidin Channels†

Anna E. Daily,‡ Jung H. Kim,§ Denise V. Greathouse,‡ Olaf S. Andersen,*,§ and Roger E. Koeppe II*,‡

‡*Department of Chemistry and Biochemistry, University of Arkansas, Fayetteville, Arkansas 72701, and* §*Department of Physiology and Biophysics, Weill Cornell Medical College, New York, New York 10065*

*Received May 27, 2010; Revised Manuscript Received July 9, 2010*

ABSTRACT: To explore the consequences of burying polar, hydrogen-bonding hydroxyl groups within the hydrocarbon core of lipid bilayer membranes, we examined the structural and functional effects of alanine-to-serine substitutions in bilayer-spanning gramicidin channels. A native Ala was replaced by Ser at position 3 or 5 in the gramicidin A (gA) sequence: formyl-VG$^2$A$^3$LA$^5$VVWLWLWLW-ethanolamide (D-residues underlined). In the head-to-head dimers that form the conducting, membrane-spanning gA channels, these sequence positions are located near the lipid bilayer center (and subunit interface). The sequence substitutions at positions 3 and 5 were tested within the context of having either Gly or D-Ala at position 2, because D-Ala$^2$ causes the channel lifetimes to increase 3-fold relative to Gly$^2$ [Mattice et al. (1995) *Biochemistry 34*, 6827]. Size-exclusion chromatograms and circular dichroism spectra show that the Ala → Ser replacements are well tolerated and have little effect on channel structure. In planar bilayers, the Ser-substituted gramicidins form well-defined channels, with cation conductances that are ~60% of those of the reference channels. The Ser-substituted channels are structurally equivalent to native gramicidin channels, as demonstrated by the formation of heterodimeric channels between a Ser-containing subunit and a native gramicidin subunit. These hybrid channels exhibit rectification, attributable to asymmetric placement of the single Ser hydroxyl group with respect to the bilayer center. Compared to the corresponding Ala-containing reference channels, the polar Ser residues decrease the analogues' channel-forming potency by 3 orders of magnitude, indicating a substantial energetic penalty (~15 kJ/mol) for burying the polar Ser side chain in the bilayer hydrophobic core.

The diverse methods used to characterize the hydrophobicities of amino acid side chains, e.g., refs (*1*−*6*), have sometimes led to contradictory results. Some of the differences may reflect the importance of knowing the amino acid side chain positions in a lipid bilayer, since the free energy profiles for moving polar side chains through the bilayer may vary substantially (*4*, *7*, *8*). Small molecule partition studies therefore may provide different information from studies where a side chain is fixed at a particular position within the bilayer. Indeed, tryptophan substitutions in gramicidin (gA)[1] channels (*9*), where the side chain positions were fixed by linkage to the bilayer-spanning channel, enabled the identification of an energetic penalty for burying the amphipathic tryptophan indole side chains in the bilayer hydrophobic core.

Because much is known about gA channels (*10*, *11*), they have become powerful tools to study the effects of amino acid sequence changes on properties such as channel folding, channel−bilayer interactions, and ion permeability. The functional changes are deduced from the channel-forming potency, folding, structure, single-channel lifetime, and monovalent cation conductance of sequence-substituted analogues. The polypeptide backbone lines the pore of the gA channel, where the carbonyl oxygens contact the permeating cations, while the hydrophobic amino acid side chains project to the outside and interact with bilayer lipids. Although the side chains are not in direct contact with the permeating cations, polar side chains still can modulate the single-channel conductance, primarily by means of through-space dipole−cation interactions (*12*) (*13*, *14*).

In this study, we focus on the introduction of serine, with its polar hydroxyl group, into the bilayer-spanning gA channels. Ser was introduced in place of Ala at position 3 or position 5 in the gA sequence: formyl-VG$^2$A$^3$LA$^5$VVWLWLWLW-ethanolamide (D-residues underlined). Because the local sequence context may modulate the effects of a sequence substitution, each Ala → Ser-substituted analogue was prepared with either D-Ala or Gly at position 2. D-Ala at position 2 increases gA channel lifetimes 3-fold and was included because D-Ala$^2$ might magnify the effects and allow the influence of the Ser substitutions to be more easily observed and evaluated (*15*).

Position 3 was chosen as a site for placement of the Ser hydroxyl side chain because its location in the dimeric gA channel places it near the center of a lipid bilayer, with the side chains of each monomer at position 3 in approximate apposition in the conducting dimer (Figure 1). Position 5 also is buried within the lipid bilayer core, but the side chains at position 5 in the two subunits are located on opposite sides of the folded channel (Figure 1), such that these side chains are not in close contact.

†This work was supported in part by NIH Grants GM070971 and RR15569 and by the Arkansas Biosciences Institute.

*To whom correspondence should be addressed. R.E.K.: e-mail, rk2@uark.edu; phone, 479-575-4976; fax, 479-575-4049. O.S.A.: e-mail, sparre@med.cornell.edu; phone, 212-746-6350; fax, 212-746-8678.

[1]Abbreviations: Boc, *tert*-butoxycarbonyl; CD, circular dichroism; DCM, dichloromethane; DMF, dimethylformamide; DMPC, 1,2-dimyristoylphosphatidylcholine; DOPC, 1,2-dioleoylphosphatidylcholine; DPhPC, 1,2-diphytanoylphosphatidylcholine; DS, double stranded; gA, gramicidin A; HPLC, high-performance liquid chromatography; NMP, *N*-methylpyrrolidone; Otbu, *tert*-butyl; SEC, size-exclusion chromatography; SS, single stranded; TFA, trifluoroacetic acid.

 Published on Web 07/13/2010 

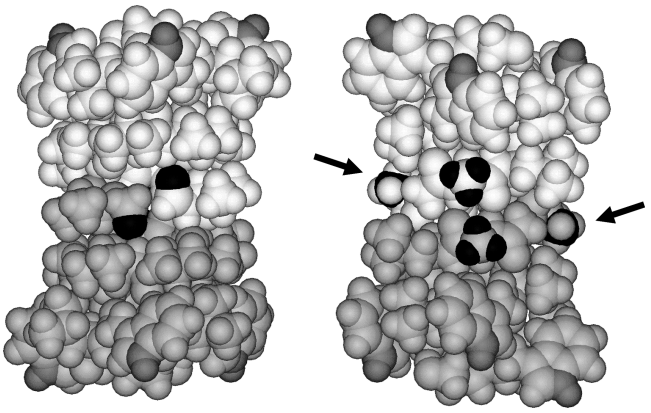

FIGURE 1: Positions of the Ala → Ser substitutions (at $Ala^3$ and $Ala^5$) in the gA channels. The CPK models show the front (left) and back (right) views of the dimeric $\beta^{6.3}$-helical channel. The two subunits are shaded in gray and white, respectively. In the front view (left), the formyl oxygens at the subunit interface are in black. In the back view (right), the $\beta$-hydrogens of the apposing $Ala^3$ methyl side chains are in black; the $\beta$-carbons of the more distal $Ala^5$ methyls are also in black (arrows). Indole ring NH groups are depicted using a somewhat darker shade of gray.

We evaluated the structural and functional properties of these Ser → Ala-substituted gA channel analogues using CD spectroscopy, size-exclusion chromatography, and single-channel analysis. We find that Ala → Ser substitutions are tolerated but that the more polar Ser side chains cause the conducting channels to form less readily, thereby reducing the analogues' channel-forming potency. The Ser side chains also reduce the single-channel lifetimes and conductances, but the major effect is the decrease in the channel-forming potency. Further, because the conducting channels are dimers (Figure 1), homodimeric Ser-substituted channels have two buried hydroxyl groups, whereas heterodimeric channels have a buried hydroxyl on *only one* subunit. We are thus able to evaluate the consequences of having two versus having one Ser side chain buried in the lipid bilayer hydrophobic core and, by comparing the properties of $Ser^3$- and $Ser^5$-substituted gA heterodimeric and homodimeric channels, to assess the possible importance of side chain hydrogen bonding in the bilayer core.

## MATERIALS AND METHODS

All chemical and reagents were of the highest grade available. Water was doubly deionized Milli-Q water.

*Peptide Synthesis*. The amino acid sequences of the analogues used in this study are listed in Table 1.

Because of the need to protect the serine side chains, the usual procedures (*16*) for synthesizing gramicidins were modified. The peptides were prepared by Fmoc solid-phase methods on an ABI 433A automated peptide synthesizer (PE Biosystems, Foster City, CA) equipped with a UV monitor. The Fmoc-amino acids from Novabiochem (EMD Biosciences, Inc., San Diego, CA) were coupled using a 5-fold excess of hydroxybenzotriazole esters in the presence of 2-(1*H*-benzotriazol-1-yl)-1,1,2,3-tetramethyluronium hexafluorophosphate to a preloaded Fmoc-Trp(Boc)-Wang resin (0.1 mmol, 0.59 mmol/g), also from Novabiochem. The side chain protecting groups were *tert*-butoxycarbonyl (Boc) for Trp and *tert*-butyl (Otbu) for Ser residues in the sequences. Peptide synthesizer reagents were from Applied Biosystems by Life Technologies, except dichloromethane (DCM) and *N*-methylpyrrolidone (NMP), which were Burdick and Jackson HPLC grade (VWR Chemical, Irving, TX). At each step, Fmoc deprotection was accomplished using 20% piperidine in NMP.

Each resin-bound peptide was treated with a solution of *p*-nitrophenyl formate (80 mg, 0.48 mmol) in 2.5 mL of cold dimethylformamide (DMF) with 10 $\mu$L of *N*-methylmorpholine to formylate the N-terminal valine residue. This suspension was mixed for 24 h in darkness at 4 °C. Following formylation, the resin was rinsed five times with 2.5 mL each of DMF, methanol, DCM, and again DMF. The completed peptide was then cleaved from the resin during a 48 h reaction at 25 °C using 2 mL of ethanolamine in 8 mL of DMF (*16*). To recover the peptide following the treatment with ethanolamine, the resin was filtered and washed five times each with DMF, DCM, and methanol. The volume of the combined filtrate and washings was then reduced to approximately 2 mL by rotary evaporation, and the peptide was precipitated by the addition of 5 volumes of $H_2O$ at 4 °C, filtered, and dried to a white powder under vacuum. Finally, to remove the protecting Boc from Trp and Otbu from Ser, the peptide was treated with trifluoroacetic acid (TFA)−DCM−phenol−triisopropylsilane−$H_2O$ (60:25:5:5:5) under $N_2$ for 1 h at 25 °C .

After 1 h, the TFA and other solvents were removed by evaporation under a stream of $N_2$. The peptide was then precipitated by addition of 0.3 mL of cold methanol and 0.3 mL of cold $H_2O$ on ice and pelleted using an Eppendorf 5451C centrifuge at 12000 rpm for 5 min at 23 °C. The pellet was washed with 0.6 mL of cold 50% methanol/water (on ice) and centrifuged three more times. After the final wash, the supernatant was removed and the pellet dried under vacuum (0.005 mmHg) overnight. The peptide was dissolved in methanol, quantified using the Trp absorbance at 280 nm (extinction coefficient ($\varepsilon$) of 5600 $M^{-1}$ $cm^{-1}$ $Trp^{-1}$ (22400 $M^{-1}$ $cm^{-1}$ $gA^{-1}$)), and analyzed by reversed-phase HPLC and electrospray ionization mass spectrometry.

*Circular Dichroism Spectroscopy and Size-Exclusion Chromatography*. Gramicidin/lipid dispersions (molar ratio 1/30) were prepared for circular dichroism (CD) spectroscopy and size-exclusion chromatography (SEC) based on methods described in ref *17*. A lipid sample consisting of 3.75 $\mu$mol of DMPC or DOPC (Avanti Polar Lipids, Alabaster, AL) in a chloroform stock solution was codissolved with 0.125 $\mu$mol of gA analogue in methanol, such that the final volumes of methanol and chloroform were equal. Samples were dried under vacuum (0.005 mmHg, with liquid $N_2$ trap) for 48 h to remove traces of solvents. Next, 0.5 mL of water was added to each sample, and samples were sonicated at 50 °C for 1 h using a Branson W-185 cell disrupter operating at a power of 30 W. After sonication, samples were placed in a heat block at 50 °C for 1 h. Following centrifugation at 12000 rpm for 5 min, the supernatant was removed and the amount of gA quantified based on the peptide absorbance at 280 nm (see above).

The undiluted supernatant was used for SEC measurements. SEC was performed at room temperature using an Ultrastyragel size-exclusion column (7.8 × 300 mm column of 7 $\mu$m beads with 0.1 $\mu$m pores; Waters Corp., Milford, MA) to determine the fraction of double-stranded (DS) versus single-stranded (SS) gA conformers. A 5 $\mu$L aliquot of each sample was injected and eluted using tetrahydrofuran (HPLC grade, from VWR) at a flow rate of 1 mL/min, ~500 psi.

Samples for CD spectroscopy were prepared by diluting the stock samples (as prepared for SEC) with water to a final concentration of 80−200 $\mu$M gramicidin. CD measurements

Table 1: Sequences of Gramicidin Analogues and Their Channel-Forming Potencies

| analogue | sequence[a] | MW | nominal concn (pM) | potency |
|---|---|---|---|---|
| [Gly$^2$]gA | formyl-VGALAVVVWLWLWLW-e | 1879 | $2 \pm 1$ | 1 |
| [Gly$^2$,Ser$^3$]gA | formyl-VGSLAVVVWLWLWLW-e | 1895 | $1200 \pm 500$ | 0.002[b] |
| [Gly$^2$,Ser$^5$]gA | formyl-VGALSVVVWLWLWLW-e | 1895 | $2100 \pm 700$ | 0.001[b] |
| [D-Ala$^2$]gA | formyl-VAALAVVVWLWLWLW-e | 1893 | $2 \pm 1$ | 1 |
| [D-Ala$^2$,Ser$^3$]gA | formyl-VASLAVVVWLWLWLW-e | 1909 | $360 \pm 40$ | 0.006[c] |
| [D-Ala$^2$,Ser$^5$]gA | formyl-VAALSVVVWLWLWLW-e | 1909 | $120 \pm 70$ | 0.02[c] |

[a]D-Amino acid residues are underlined; "e" denotes ethanolamide; "MW" denotes the expected monoisotopic molecular mass, in Daltons (without $^{13}$C). "Nominal concentration" denotes the concentration needed to observe a channel appearance rate ~1/s. These numbers are accurate to within a factor of 2 to 3. [b]The channel-forming potency is calculated relative to native [Gly$^2$]gA. The potency is based upon the reciprocal of the relative molar amount of analogue needed to achieve about one channel event s$^{-1}$. [c]The channel-forming potency is calculated relative to [D-Ala$^2$]gA, which has a channel-forming potency similar to that of [Gly$^2$]gA.

were performed at room temperature using a Jasco 710A spectrometer. Each displayed spectrum is the average of 12 scans, obtained using a 0.1 cm path length, 1.0 nm bandwidth, 0.2 nm step resolution, and a scan speed of 20 nm/min.

*Peptide Purification*. Prior to single-channel analysis, the gA analogues were twice purified using two Zorbax-C8 (4.6 × 25 mm) columns of 5 $\mu$m octyl-silica (Mac-Mod Analytical, Chadds Ford, PA). The analogues were eluted using 84% methanol plus 0.1% TFA in water. Samples collected from the first column were repurified on a second column, as described previously (*18*). In each case, only the material eluting between 90% and 100% of the peak absorbance at 280 nm was collected, thereby eliminating the leading edge or trailing tail of a peak. These purified analogues (concentration 0.2−0.3 $\mu$M) were used for the electrophysiology studies.

*Electrophysiology*. Single-channel measurements were performed using planar bilayers formed from 2.5% (w/v) diphytanoylphosphatidylcholine (DPhPC) in *n*-decane in a Teflon partition (~1.5 mm diameter) that separates two aqueous solutions of unbuffered 1.0 M CsCl or 1.0 M NaCl. All experiments were done at 25 ± 1 °C using the bilayer punch technique (*19*). The gA analogues were twice purified (see above). Except where noted, the analogues were added symmetrically to both sides of the bilayer. The amount of twice-purified analogue that was added in each experiment was adjusted to give approximately one channel appearance per second, with the reciprocal of this amount being used to calculate the relative channel-forming potency. Single-channel current amplitude histograms and lifetime histograms were constructed as described in refs *20* and *15*. Single-channel lifetimes ($\tau$) were determined by fitting a single exponential distribution ($N(t)/N(0) = \exp\{-t/\tau\}$, where $N(t)$ is the number of channels with lifetimes longer than time $t$) to the survivor histogram of the gramicidin channel lifetime distribution.

## RESULTS

All four Ala → Ser-substituted gA analogues examined here are able to form cation-conducting channels (see below). The Ser$^5$ substitutions, which are more distal from each other (Figure 1), are less perturbing than are the Ser$^3$ substitutions. We convey first the results for the Ser$^3$ gramicidins.

*Ala$^3$ → Ser$^3$ Mutation*. (*A*) *Channel Fold and Subunit Stoichiometry*. Because the residue 3 side chains could be rather crowded next to each other in the membrane-spanning gA channel (Figure 1), it became important to determine the extent to which Ser$^3$ gA analogues could fold and assemble as transmembrane dimers. When examined by either CD or SEC, the observed population of [Ser$^3$]gA conformers consists predominantly of SS monomers which assemble into transmembrane dimers in DMPC or DOPC, regardless of the identity of residue 2, whether Gly$^2$ or D-Ala$^2$.

The CD spectra for [Gly$^2$,Ser$^3$]gA and especially [D-Ala$^2$,Ser$^3$]gA in DMPC vesicles (Figure 2A) are characteristic of the standard, right-handed (RH), single-stranded (SS) $\beta^{6.3}$-helical conformation typical of the gA channel (*17*), indicating that the polar Ser residues have been successfully buried within the DMPC acyl chains near the bilayer center (*21*, *22*). The spectrum for [Gly$^2$,Ser$^3$]gA exhibits somewhat lower positive ellipticity at 220 nm along with a more negative trough near 230 nm, suggestive of (some) conformational polymorphism wherein the analogue can fold into the RH, SS $\beta^{6.3}$-helical dimer as well as smaller amounts of DS conformers. Size-exclusion chromatography (Figure 2B) confirms that about 90% of [D-Ala$^2$,Ser$^3$]gA and 75% of [Gly$^2$,Ser$^3$]gA are present as the SS $\beta^{6.3}$-helical conformation in DMPC. In both cases the leading DS peak is smaller than the major peak representing the SS conformation. In DOPC there is a modest increase, from ~10% to ~20%, in the DS population of [D-Ala$^2$,Ser$^3$]gA, compared to DMPC, although no change for [Gly$^2$,Ser$^3$]gA.

(*B*) *Channel Functional Properties*. When examined electrophysiologically, single-channel experiments with either [Gly$^2$,Ser$^3$]gA or [D-Ala$^2$,Ser$^3$]gA reveal a single predominant conducting channel type, as evident in the single-channel current traces (Figure 3). The current transition amplitude histograms and single-channel lifetime distributions (not shown) similarly provide evidence for the existence of a single predominant conducting channel structure.

The Ala → Ser substitution (panels C and D of Figure 3) reduced the single-channel conductances by about 40% relative to the corresponding Ala$^3$ gAs (panels A and B); the results are summarized in Table 2.

The substitutions similarly reduced the single-channel lifetimes by 3−5-fold for channels with D-Ala or Gly at position 2, respectively; the results are summarized in Table 3. The major consequence of the Ala → Ser substitution, however, is that we needed to add 100−1000-fold more of the Ser-substituted gA analogues, relative to the Ala-containing counterparts, in order to observe comparable single-channel appearance rates. The Ser-substituted gA analogues thus have 100−1000-fold lower channel-forming potencies (Table 1). These decreases in single-channel lifetime and channel-forming potency should be expected because we introduced polar residues at the subunit interface near the lipid bilayer center.

The consequences of an Ala → Ser substitution at position 3 depend on the identity of the residue at position 2. As might have been expected from the CD and SEC results (Figure 2), the

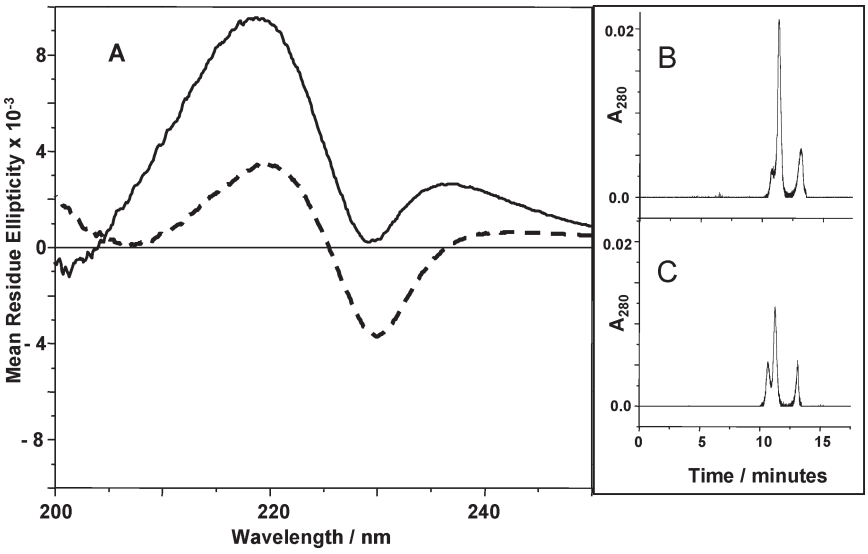


FIGURE 2: Circular dichroism and size-exclusion experiments on $Ala^3 \rightarrow Ser^3$-substituted gramicidins. (A) CD spectra for [D-$Ala^2$,$Ser^3$]gA (—) and [$Gly^2$,$Ser^3$]gA (- - -) in DMPC vesicles. (B, C) Size-exclusion chromatograms for (B) [D-$Ala^2$,$Ser^3$]gA and (C) [$Gly^2$,$Ser^3$]gA in DMPC vesicles. (The peaks at ~10.5 min represent DS conformers, the peaks at ~12 min represent monomers, and the final peaks at ~13 min are due to lipids, not peptide.)

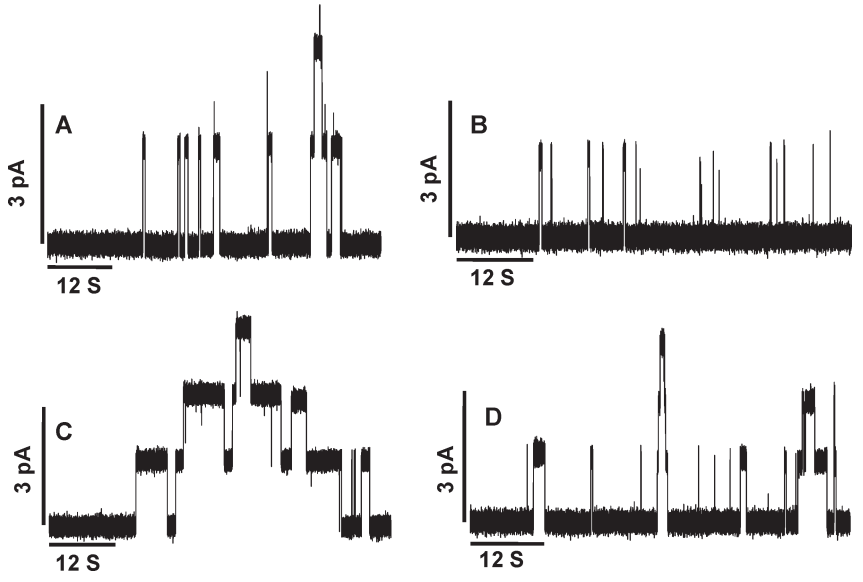


FIGURE 3: Single-channel current traces channels formed by Ala → Ser-substituted gramicidin analogues. (A) [D-$Ala^2$,$Ser^3$]gA; average channel current, $g$ = 2.2 pA; mean channel lifetime, $\tau$ = 1200 ms. (B) [$Gly^2$,$Ser^3$]gA; $g$ = 1.8 pA; $\tau$ = 110 ms. (C) [D-$Ala^2$,$Ser^5$]gA; $g$ = 1.7 pA; $\tau$ = 4000 ms. (D) [$Gly^2$,$Ser^5$]gA; $g$ = 1.5 pA; $\tau$ = 900 ms. Conditions: 1.0 M NaCl, DPhPC/*n*-decane, 200 mV.

Table 2: Single-Channel Current Transition Amplitudes for Channels Formed by Different Combinations of Ser and Ala Gramicidin Subunits[a]

| subunit A | subunit B | $i_{AA}$ (pA) | $i_{AB}$ (pA) | $i_{BA}$ (pA) | $i_{BB}$ (pA) |
|---|---|---|---|---|---|
| [$Gly^2$,$Ser^3$]gA | gA | 1.8 | 2.1 | 2.5 | 3.0 |
| [D-$Ala^2$,$Ser^3$]gA | [D-$Ala^2$]gA | 2.2 | 2.6 | 3.0 | 3.7 |
| [$Gly^2$,$Ser^5$]gA | gA | 1.5 | 1.8 | 2.4 | 3.2 |
| [D-$Ala^2$,$Ser^5$]gA | [D-$Ala^2$]gA | 1.7 | 2.2 | 2.8 | 3.5 |

[a]For the hybrid channel experiments, both subunit types were added to both sides of a planar bilayer membrane. The current transition amplitudes for the asymmetric channel types, $i_{AB}$ and $i_{BA}$, denote the direction of the cation flow (from subunit A to subunit B, and vice versa). The direction of current flow was determined in experiments where the two gA analogues were added asymmetrically to opposite sides of the bilayer (see Figure 6). Conditions: 1.0 M NaCl, DPhPC/*n*-decane, 200 mV.

relative lifetime changes are greater for [$Gly^2$,$Ser^3$]gA than for [D-$Ala^2$,$Ser^3$]gA channels, and the channel-forming potency of [$Gly^2$,$Ser^3$]gA is less than that of [D-$Ala^2$,$Ser^3$]gA (Table 1). Nevertheless, the average single-channel current transition amplitudes are similar for [$Gly^2$,$Ser^3$]gA or [D-$Ala^2$,$Ser^3$]gA channels (1.8 and 2.2 pA, Table 2).

The electrophysiological experiments were done in DPhPC/*n*-decane bilayers, which have been used in many previous studies on amino acid-substituted gA analogues (*12*, *23*−*26*). The acyl chain composition thus differs from the DMPC and DOPC bilayers that were used for the CD and SEC experiments. The gAs' conformational preference, however, varies only little with changes in the acyl chain length of the bilayer-forming lipids (as long as $10 \leq n \leq 20$ (*17*, *27*)), meaning that it is possible to compare the results of the electrophysiological and CD and SEC experiments.

*$Ala^5 \rightarrow Ser^5$ Mutation. (A) Channel Folding and Subunit Stoichiometry*. The $Ala^5 \rightarrow Ser^5$ mutation effects on gA channel folding and function are less pronounced than is the case

Table 3: Lifetimes of Symmetric and Heterodimeric Channels Formed between the Ser-Containing gA Analogues and Ala-Containing Reference Analogues[a]

| subunit A | subunit B | $r_{hybrid}$ | $\tau_{AA}$ (ms) | $\tau_{BB}$ (ms) | $\tau_{AB}$ (ms) | $\tau_{BA}$ (ms) | $\tau_{hybrid}$ |
|---|---|---|---|---|---|---|---|
| [Gly$^2$,Ser$^3$]gA | [Gly$^2$,Ala$^3$]gA | 1.08 | 139 ± 2 | 736 ± 3 | 289 ± 2 | 319 ± 2 | 0.95 |
| [D-Ala$^2$,Ser$^3$]gA | [D-Ala$^2$,Ala$^3$]gA | 1.05 | 1093 ± 10 | 3094 ± 17 | 1710 ± 10 | 1534 ± 10 | 0.88 |
| [Gly$^2$,Ser$^5$]gA | [Gly$^2$,Ala$^5$]gA | 0.95 | 397 ± 5 | 534 ± 3 | 490 ± 4 | 546 ± 4 | 1.12 |
| [D-Ala$^2$,Ser$^5$]gA | [D-Ala$^2$,Ala$^5$]gA | 0.99 | 3800 ± 30 | 3570 ± 30 | 3610 ± 30 | 3930 ± 30 | 1.02 |

[a]Subunits A and B were both added to both sides of a planar bilayer membrane. The relative appearance rate, $r_{hybrid}$, is defined in eq 1, where $n_{AA}$, $n_{BB}$, $n_{AB}$, and $n_{BA}$ are the respective numbers of channels observed for the various homo- and heterodimer combinations of subunits A and B (*25*, *26*). $\tau_{AA}$, $\tau_{BB}$, $\tau_{AB}$, and $\tau_{BA}$ are the respective single-channel lifetimes, in ms, for the various homo- and heterodimer combinations of subunits A and B. The relative lifetime ratio, $\tau_{hybrid}$, is defined in eq 3. (Gly$^2$, Ala$^3$, and Ala$^5$ are listed only for emphasis, as these are the natural residues in gA from *B. brevis*.)

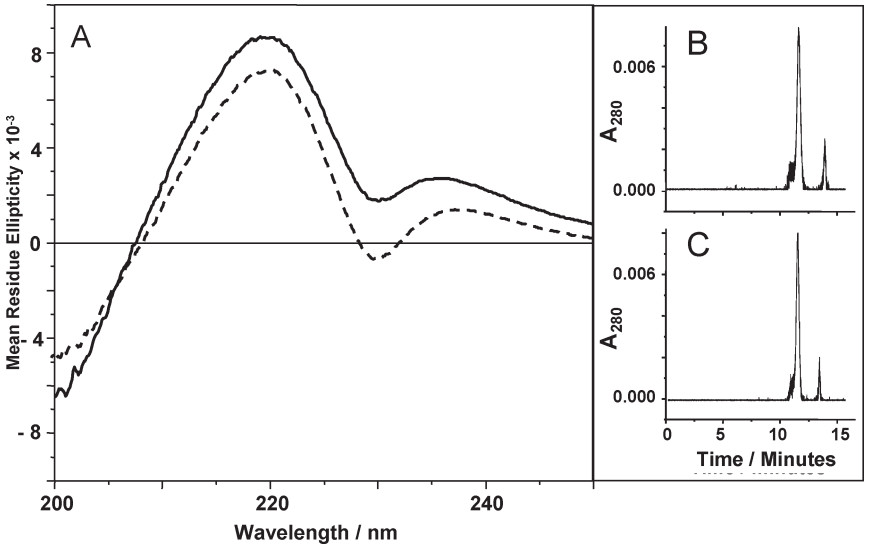


FIGURE 4: Circular dichroism and size-exclusion experiments on Ala$^5$ → Ser$^5$-substituted gramicidins. (A) CD spectra for [D-Ala$^2$,Ser$^5$]gA (—), and [Gly$^2$,Ser$^5$]gA (- - -) in DMPC vesicles. (B, C) Size-exclusion chromatograms for (B) [D-Ala$^2$,Ser$^5$]gA and (C) [Gly$^2$,Ser$^5$]gA in DMPC vesicles. (The final peak is due to lipids, not peptide.)

for the Ser$^3$ mutations. Figure 4 shows the CD and SEC results for the Ser$^5$ mutants.

The CD spectra show that an Ala → Ser mutation at position 5 has little effect on the channel structure in DMPC (Figure 4A) or DOPC. The spectra for not only [D-Ala$^2$,Ser$^5$]gA but also [Gly$^2$, Ser$^5$]gA are quite similar to that of the native gA SS channel conformation. The Ser$^5$ analogues retain primarily the SS channel conformation, in spite of the apparent need to bury both of the polar Ser$^5$ side chains among the lipid acyl chains (Figure 1) when the subunits come together. The SEC results confirm the presence of the SS conformation for both Ser$^5$ analogues (Figure 4B,C), with only ~10% DS conformers in each case. Similar results were obtained in DOPC.

(*B*) *Channel Functional Properties*. Compared to the Ser$^3$ analogues, the Ser$^5$ gA analogues form channels that have much longer lifetimes and slightly lower single-channel current transitions (Figure 3, Table 2). These trends remain true whether the identity of residue 2 is Gly$^2$ or D-Ala$^2$. The longer single-channel lifetimes appear to be directly related to the serine positions. When the Ser side chains abut each other, in the Ser$^3$ gramicidins, the lifetimes (Table 3) are much shorter than when the Ser side chains are approximately on opposite sides of the channel axis (Figure 1), as in the Ser$^5$ gramicidins. Although serine at either position reduces the single-channel conductance (Table 2), the serine position in the sequence is much less important for the single-channel conductances than for the lifetimes. As was the case the position 3 mutations, the major consequence of the Ala → Ser mutation is the reduced channel-forming potency (Table 1).

*Heterodimer Experiments*. The properties of the Ala → Ser-substituted gA subunits were investigated further in heterodimer experiments. These experiments allow for tests of whether a sequence-substituted gA analogue forms channels that are structurally equivalent to native gA channels and whether the sequence substitution stabilizes or destabilizes a conducting dimeric channel (*25*, *28*). This test for structural equivalence can be accomplished because gA channels are symmetric, antiparallel dimers and gA analogues form only one conducting channel type (*10*, *25*). In heterodimer or hybrid channel experiments, a gA analogue and a reference gA are added to both sides of a bilayer, and one examines the pattern of channel formation. Let the two gA analogues be denoted A and B; then one would expect to observe up to four different channel types: two homodimers, AA and BB, if the homodimeric channels have different conductances, and one or two heterodimeric channel types.

Relative to the polarity of the applied potential, two different hybrid channel combinations are possible (AB and BA). They can be distinguished if their current transition amplitudes differ from those of the parent homodimeric channels (AA and BB) and from each other, namely, if the energy barrier to ion movement through the heterodimeric channels is sufficiently asymmetric that the magnitude of current flow in the A → B direction is different from that in the B → A direction.

In these experiments, each of the Ser-substituted gA analogues was examined together with the equivalent reference Ala gA analogue, coexisting in the same bilayer membrane, such that the pair of subunits in each heterodimer experiment differed by only the single-site Ser/Ala "mutation". In these heterodimer

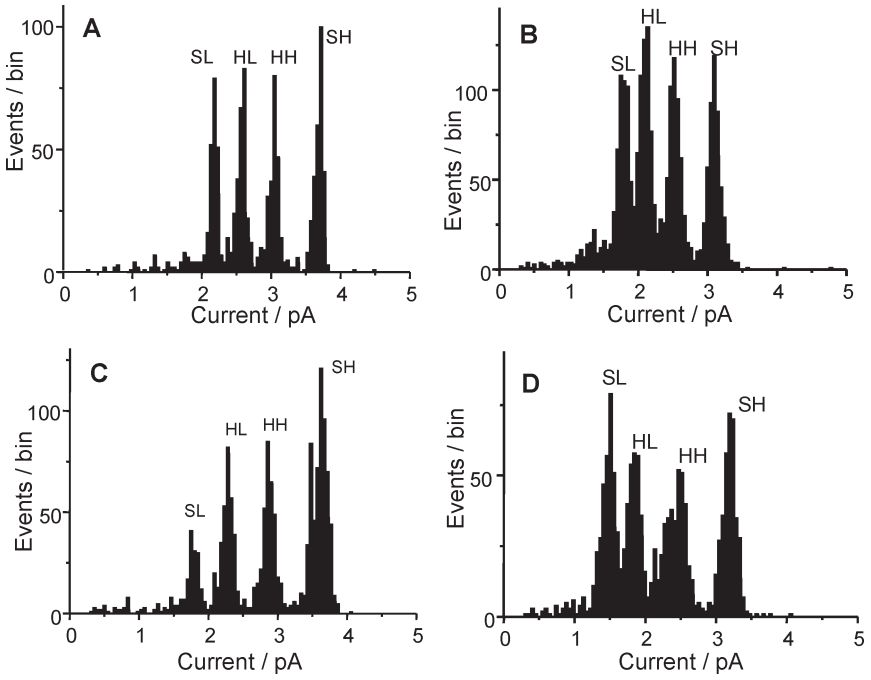


FIGURE 5: Single-channel current transition amplitude histograms for heterodimer experiments involving $Ser^3/Ala^3$ and $Ser^5/Ala^5$ gA subunit combinations. In each experiment, both subunits were added to both sides of a planar bilayer. The subunit combinations were (A) [D-$Ala^2$,$Ser^3$]gA with [D-$Ala^2$,$Ala^3$]gA, (B) [$Gly^2$,$Ser^3$]gA with [$Gly^2$,$Ala^3$]gA, (C) [D-$Ala^2$,$Ser^5$]gA with [D-$Ala^2$,$Ala^5$]gA, and (D) [$Gly^2$,$Ser^5$]gA with [$Gly^2$,$Ala^5$]gA. The peaks designated SL and SH denote the symmetric low-conductance (Ser-substituted) and high-conductance (reference) channels; HL and HH denote the low- and high-conductance heterodimeric channels. Conditions: 1.0 M NaCl, 200 mV.

experiments, with subunit pairs differing in $Ser^3/Ala^3$ or $Ser^5/Ala^5$, each with a (constant) $Gly^2$ or D-$Ala^2$, we observed the expected four different conductance levels, corresponding to the AA, AB, BA, and BB subunit combinations. The single-channel current transition amplitude histograms with the different combinations are shown in Figure 5.

In each experiment, the two distinct hybrid channel peaks arise because the serine residue is off center within the heterodimer, which leads to different ion currents in the two directions through the hybrid channels.

The direction of the current with respect to the subunit orientation in the hybrid channels was determined in experiments where the different subunits were added asymmetrically to different sides of a bilayer. Figure 6 illustrates the results of such an experiment using subunits of [$Gly^2$,$Ser^3$]gA and [$Gly^2$,$Ala^3$]gA.

In each panel of Figure 6, there are two peaks, a dominant heterodimer peak, plus a minor peak representing the symmetric Ala-containing reference gA analogue. (Though gA crosses lipid bilayers poorly (*29*), it can do so to a minor extent.) The panels in the figure show that the current is higher when $Na^+$ ions enter the $Ala^3$ subunit and then cross the bilayer center to the $Ser^3$ subunit than in the other direction. This finding held true for each combination of subunits in all of the Ser/Ala heterodimeric channels, regardless of whether residue 3 or residue 5 was modified. The single-channel currents are summarized in Table 2.

When the homo- and heterodimeric channels are observed in a single experiment in the same bilayer, it becomes feasible and meaningful to assess the relative channel appearance rates ($r_{hybrid}$) for forming heterodimeric channels relative to the homodimeric channels, which can be determined from the numbers of single-channel transitions in the different populations:

$$r_{hybrid} = \sqrt{\frac{n_{AB}n_{BA}}{n_{AA}n_{BB}}} \quad (1)$$

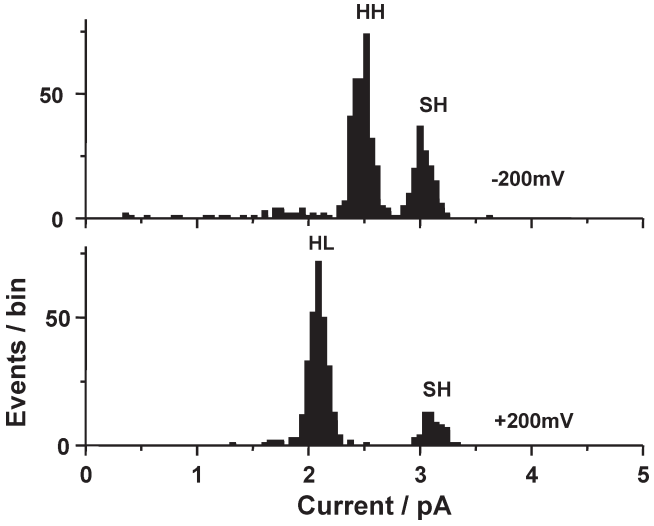


FIGURE 6: Single-channel current transition amplitude histograms obtained after asymmetric addition experiments involving [$Gly^2$,$Ser^3$]gA and [$Gly^2$,$Ala^3$]gA subunits. Each subunit was added to only one side of a planar lipid bilayer, with the [$Gly^2$,$Ala^3$]gA-containing solution being the electrical reference. At −200 mV applied potential, when the $Na^+$ ions move from the [$Gly^2$,$Ala^3$]gA to the [$Gly^2$,$Ser^3$]gA subunit, the high-conducting heterodimeric (HH) channels were observed. At +200 mV applied potential, when the $Na^+$ ions move from the [$Gly^2$,$Ser^3$]gA to the [$Gly^2$,$Ala^3$]gA subunit, the low-conducting heterodimeric (HL) channels were observed. Because the native [$Gly^2$,$Ala^3$]gA subunits have a high channel-forming propensity (and cross the membrane, albeit slowly (*29*)), some symmetric, homodimeric [$Gly^2$,$Ala^3$]gA channels (SH) are observed at both potentials.

where $n_{AA}$, etc., denote the number of each channel type observed in a given experiment. (Because each channel type is observed in the same recording, and both subunits are added to both sides of the bilayer, the number of channels observed is proportional to

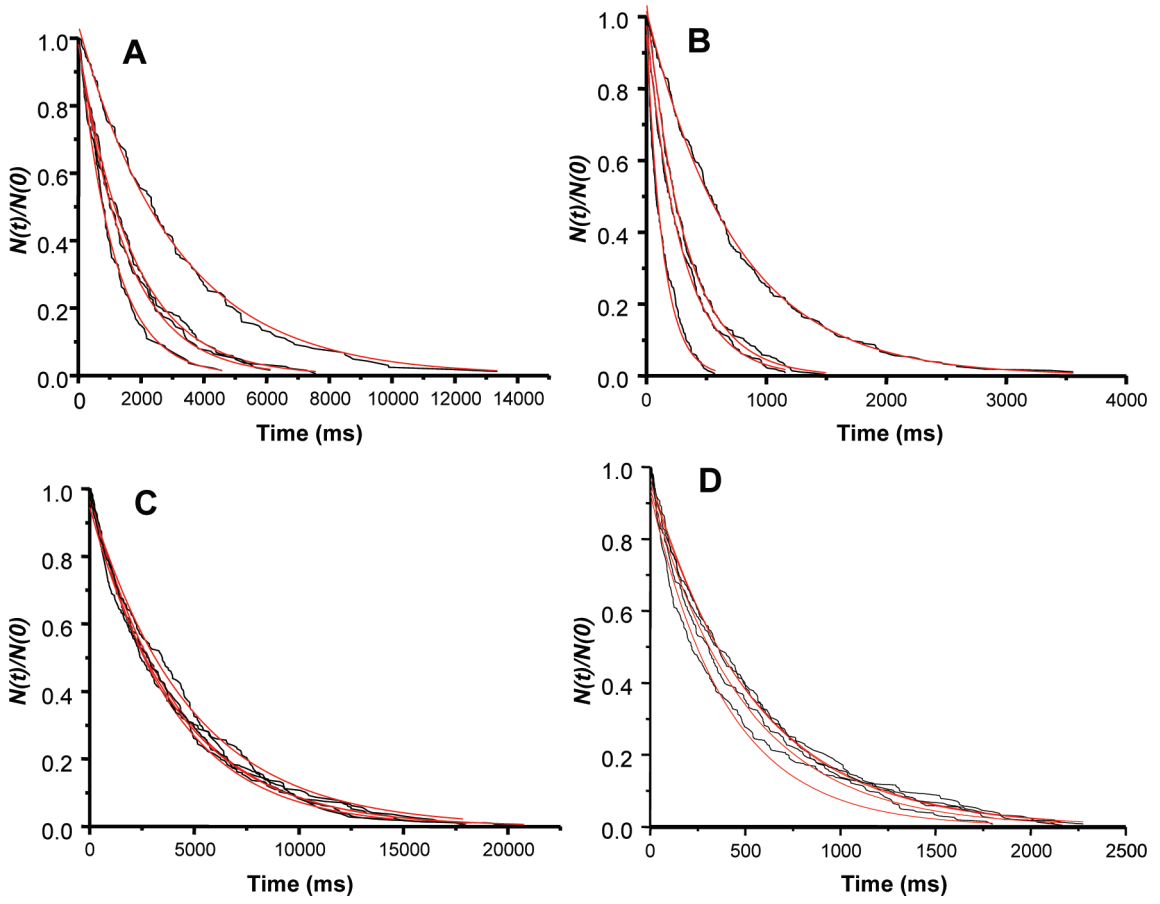


FIGURE 7: Channel lifetime histograms for heterodimer experiments. In each experiment, both subunits were added to both sides of a planar bilayer membrane. The subunit combinations were (A) [D-Ala$^2$,Ser$^3$]gA with [D-Ala$^2$,Ala$^3$]gA, (B) [Gly$^2$,Ser$^3$]gA with [Gly$^2$,Ala$^3$]gA, (C) [D-Ala$^2$,Ser$^5$]gA with [D-Ala$^2$,Ala$^5$]gA, and (D) [Gly$^2$,Ser$^5$]gA with [Gly$^2$,Ala$^5$]gA. Each survivor distribution was fit by a single-exponential distribution (depicted by the smooth curves). Conditions: 1.0 M NaCl, 200 mV.

the appearance frequency.) For the Ser$^3$-gA analogues, $r_{hybrid} \approx 1.0$ regardless of the identity of the residue at position 2 (Table 3). The association rate constant for the Ser$^3$/Ala$^3$ and Ala$^3$/Ser$^3$ heterodimeric channels therefore is comparable to what would be predicted from the geometric mean of the association rate constants for the corresponding homodimeric Ser$^3$- and Ala$^3$-gA homodimeric channels. Whether residue 2 is Gly or D-Ala, $r_{hybrid}$ is close to 1.0 (Table 3), indicating little preference for forming the heterodimeric channels over the homodimeric Ser$^3$/Ser$^3$ channels. For the Ser$^5$-gAs, $r_{hybrid}$ is also close to 1.0, again showing little preference for forming heterodimers that have Ser$^5$ in only one subunit (Table 3). Overall, apart from the decreased channel-forming potency, there is surprisingly little effect of inserting two Ser$^3$ residues in close juxtaposition near the bilayer center.

It also is possible to compare the relative single-channel lifetimes for the heterodimeric and homodimeric channels. The lifetime histograms for these experiments are shown in Figure 7, and the respective single-channel lifetimes for the various subunit combinations are summarized in Table 3. (The lifetimes of the Ala$^3$- or Ala$^5$-gA channels were not altered by the addition of the Ser$^3$- or Ser$^5$-gA channels, even though the Ser-gA analogies were present at much higher concentrations, indicating that the Ser-containing gA analogues do not alter gA channel properties.)

In the absence of subunit-specific molecular interactions, the average heterodimer lifetime should equal the geometric mean of the respective homodimer lifetimes (*25*):

$$\sqrt{\tau_{AB}\tau_{BA}} = \sqrt{\tau_{AA}\tau_{BB}} \quad (2)$$

which we quantify by the relation:

$$\tau_{hybrid} = \frac{\sqrt{\tau_{AB}\tau_{BA}}}{\sqrt{\tau_{AA}\tau_{BB}}} \quad (3)$$

wherein $\tau_{hybrid}$ is 1.0 if there is no stress at the subunit interface (*28*). This expectation holds true for both the Ser$^5$/Ala$^5$ gramicidins and the Ser$^3$/Ala$^3$ gramicidins, irrespective of the residue at position 2 (Table 3).

## DISCUSSION

In this study, we examined the consequences of Ala → Ser replacements in gramicidin channels, where the Ser residues will be located at the channel/bilayer boundary and close to the bilayer center. Our main findings are that the conducting channels formed by the Ser-containing subunits are structurally equivalent to the native gA channels; yet there is a substantial energetic penalty associated with the formation of the Ser-containing channels, as evident from the reduced channel-forming potency of the Ser-containing subunits. This reduced potency reflects the energetic cost of burying the rather polar Ser hydroxyl groups in the lipid bilayer hydrophobic core. (The combined cost arises from the needs to fold the Ser-containing gA analogues into $\beta^{6.3}$-helical subunits and to insert the folded subunits into the lipid bilayer core.) In addition, though the Ser$^3$ residues will be in close apposition in the bilayer-spanning $\beta^{6.3}$-helical channels, whereas the Ser$^5$ residues will be far part (Figure 1), there is surprisingly little difference in properties among the hetero- and

homodimeric Ser-containing channels. We first discuss the practical requirements for high-purity gA analogues, made more stringent by the low channel-forming potency. We then discuss the implications for serine hydroxyl group interactions in the hydrophobic lipid bilayer core.

*Synthesis of Ser-Containing gA Analogues*. The Ser-containing gA analogues have very low channel-forming potency (Table 1), such that a key element in this study was the ability to make available essentially pure gA analogues. Because the serine hydroxyl side chain needed to be protected during peptide synthesis and the purity requirements were high, we found it necessary to modify significantly the "usual" procedures (*16*) for the solid-phase chemical synthesis of gramicidin analogues.

All of the gA side chains are either aliphatic or tryptophan (*30*), and the solid-phase chemical synthesis of gA analogues usually does not require side-chain protecting groups (*16*); even the tryptophans do not need to be protected. This chemical stability of Trp during the "typical" synthesis of a gA analogue arises for several reasons. First, in the absence of polar amino acids, the gramicidin Trp residues are quite stable during standard acid hydrolysis of peptide bonds; more than 75% of theoretical Trp is recovered when gA is hydrolyzed in 6 N HCl at 110 °C (*31*−*33*). Second, with no protecting groups other than $N_\alpha$-Fmoc, gA can be synthesized and cleaved from a solid resin without using acid conditions (*16*). Acid can be avoided because the Fmoc groups are removed using piperidine, a mild base, and the ethanolamine serves dual roles at the conclusion of the synthesis, as both a mild base, for releasing the peptide from the resin, and as the essential C-blocking group in the finished peptide. By contrast, polar side chains such as Ser require protection. Then, because acid cleavage eventually will be employed, the Trp indole rings also need protection; and the approach to the synthesis requires modifications.

For the synthesis of the Ser-containing gA analogues, we therefore chose to release the still protected (formylated) peptides from the Wang resin using ethanolamine, which again provided the essential C-blocking group for each peptide. The Ser and Trp protecting groups were then removed from the soluble peptides using 60% TFA at 25 °C (see Materials and Methods). These procedures worked well for producing the desired products. Mass spectra revealed the expected monoisotopic *m*/*z* ratios of 1896 and 1910 for the $MH^+$ ions of the single Ser-containing and deprotected $Gly^2$ and D-$Ala^2$ analogues, respectively (see Table 1).

*Effect of Ala → Ser Substitutions on Subunit Folding and Channel Formation*. While each of the $Ser^3$ and $Ser^5$ gA analogues forms ion-conducting channels (Figure 3), the channel-forming potencies are greatly reduced. The constraints imposed by serine on subunit folding seem rather modest, being most evident in the CD spectrum and SE chromatogram for [$Gly^2$,$Ser^3$]gA (Figure 2), which nevertheless indicate the occurrence of still only ~25% DS conformers in the population. The constraints on subunit association are reflected more dramatically in the channel-forming potencies, which are reduced 2−3 orders of magnitude, in seeming conflict with the CD and SE results. (This apparent conflict could perhaps reflect the different acyl chain lengths in the different experiments. That possibility can be excluded, however, because the conformational preferences of the different gA analogues are similar in DMPC and DOPC, lipids having acyl chains lengths that bracket the acyl chain length of DPhPC.)

To reconcile these observations, we note a key difference between the CD and SE experiments and the single-channel experiments; the [Ser]gA/lipid ratio is 1/30 in the CD and SE experiments but ~1/10000 in the single-channel experiments (based upon the amounts of lipid and gA that are added to the experimental chamber). This is important because gA channels are dimers (*34*−*36*) that form by the transmembrane dimerization of subunits from each bilayer leaflet (*29*), and the $\beta^{6.3}$-helical subunits can be inserted in the lipid bilayer (*37*). Thus, assuming that Ala → Ser substitutions introduce an energetic penalty for burying the $\beta^{6.3}$-helical subunits in the bilayer core, one can approximate the channel formation by the following schemes. For the $Ala^3$- and $Ala^5$-containing subunits:

$$M + M \overset{K_A}{\leftrightarrow} D \qquad \text{(Scheme 1)}$$

where $K_A$ denotes the association constant for channel formation. In this case, the distribution between monomers and dimers can be obtained from

$$[D] = \frac{4[T]K_A + 1 - \sqrt{1 + 8[T]K_A}}{8K_A} \qquad (4)$$

in which $T$ is the total gramicidin concentration ($T = M + 2D$); see ref *30*. The expression reduces to $[D] = [T]/2$ in the limit when $[T]K_A \rightarrow \infty$, or to $[D] = [T]^2K_A$ in the limit of $[T]K_A \rightarrow 0$.

For the $Ser^3$- or $Ser^5$-containing subunits, Scheme 1 is extended to include a membrane-insertion step:

$$M' \overset{K_1}{\leftrightarrow} M'' \quad \text{and} \quad M'' + M'' \overset{K_A}{\leftrightarrow} D \qquad \text{(Scheme 2)}$$

where $M'$ and $M''$ denote gA monomers that are not inserted ($M'$) and inserted ($M''$) into the bilayer leaflet; $K_1$ is the equilibrium constant for the $M''/M'$ distribution, and $K_A$ the dimerization constant for channel formation (from $M''$ only). In this case, the distribution between monomers and dimers can be obtained from

$$[D] = \frac{4[T]K'_A + 1 - \sqrt{1 + 8[T]K'_A}}{8K'_A} \qquad (5)$$

where $K'_A = K_A K_1^2/(K_1 + 1)^2$. Equation 5 reduces to $[D] = [T]/2$ in the limit when $[T]K'_A \rightarrow \infty$, or to $[D] = [T]^2K'_A$ in the limit when $[T]K'_A \rightarrow 0$.

For the native molecule [$Gly^2$]gA, $K_A \approx 10^{14}$ cm$^2$/M in (*n*-decane-containing) DOPC (*34*, *38*) or DPhPC (*39*) bilayers. [D-$Ala^2$]gA has a similar channel-forming potency as [$Gly^2$]gA (Table 1) and a longer channel lifetime, meaning that it should have an even higher $K_A$. In DMPC bilayers, $K_A$ will be larger than the above estimate because of the thickness dependence of the gA channel stability (*34*, *40*). The CD and SE experiments were done at gA/lipid mole fractions (~1/30) much higher than $1/K_A$ (~$4 \times 10^{-5}$ in DOPC/*n*-decane bilayers when expressed in terms of the gA/lipid ratio). Under these conditions, nearly all of the gA will be $\beta^{6.3}$-helical dimers, and the destabilization due to the Ala → Ser substitutions, although present, will be difficult to detect, except in the cases of extreme destabilization, such as [$Gly^2$,$Ser^3$]gA, (cf. Figures 2 and 4).

The single-channel experiments were done at gA/lipid mole fractions about $10^{-7}$ to $10^{-6}$ (for the analogues without serine), estimated according to ref *25*, which are much lower than $1/K_A$. Under these conditions, changes in $K_A$ or $K'_A$ would be reflected as changes in the channel-forming potencies (Table 1). For the $Gly^2$ analogues, the Ala → Ser substitution causes the channel-forming potency to decrease 3 orders of magnitude while for the

D-Ala$^2$ analogues the reduction is about 2 orders of magnitude. The reduction in channel-forming potency could reflect changes in $K_I$ or $K_A$, or both. Regardless, the potencies reveal a free energy cost of about 12−18 kJ/mol for burying a Ser residue in the lipid bilayer core, relative to an Ala residue. This estimate is in good agreement with the 14 kJ/mol predicted by Radzicka and Wolfenden (*41*), based on the cyclohexane/water partition coefficient of methanol (a serine side chain mimic), the 16 kJ/mol predicted by MacCallum et al. (*4*), based on molecular dynamics simulations of amino acid side chain analogues in lipid bilayers, and the 14 kJ/mol predicted by Choe et al. (*42*), based on a continuum electrostatic model of amino acid side chains incorporated into bilayer-spanning helices; but higher than the values deduced from the octanol/water distribution of methanol, ~0 kJ/mol (*41*), or the octanol/water (*43*) or lipid bilayer/water (*44*) distributions of a series of host−guest peptides, 1−2 kJ/mol (*8*).

*Effect of Ala → Ser Substitutions on Channel Lifetimes*. As might be expected, Ala → Ser substitutions alter the single-channel lifetimes much less than the channel-forming potencies (Table 3). There exists, nevertheless, a position dependence. The Ala$^3$ → Ser$^3$ substitution diminishes the single-channel lifetime of the homodimeric channels some 3-fold (when D-Ala$^2$ is present) to 5-fold (when Gly$^2$ is present); see Figure 7 and Table 3. In contrast, Ala$^5$ → Ser$^5$ substitutions have little effect on the single-channel lifetimes (Figure 7 and Table 3). The difference presumably is due to the close proximity of the two Ser$^3$ residues from opposing subunits in the bilayer-spanning dimer (Figure 1). The lifetimes of the heterodimeric channels having only one Ser$^3$ residue nonetheless conform to the prediction of eq 2, indicating a lack of subunit-specific interactions at the dimer interface. Perhaps the Ser$^3$ hydroxyl group clashes even with the opposing Ala$^3$ side chain; alternatively, Ser$^3$ could form hydrogen bonds with the peptide backbone and thereby destabilize the dimer interface.

*Effect of Ala → Ser Substitutions on Ion Permeability*. Once the channels form, the single-channel currents are reduced some 40−50% by the Ala$^3$ → Ser$^3$ or Ala$^5$ → Ser$^5$ substitutions (Figure 2 and Table 2). Each of the Ser$^3$ gramicidin homodimers, regardless of the identity of residue two, exhibits single-channel current transitions that are ~0.6 of those of the corresponding Ala$^3$ gramicidin channels. The Ser$^5$ gramicidin channels have current transitions that are further diminished, being ~0.8 of those of the corresponding Ser$^3$ gramicidin channels. The dependence of the single-channel current reduction on the Ser side chain positions likely reflects through-space ion−dipole interactions (*12*, *23*), which will depend upon the average orientation and dynamics of each serine hydroxyl group.

It is possible to estimate the effect of the side chain dipole on ion permeability following Koeppe et al. (*12*) using the experimental dipole moment for alcohols, $\mu \approx 1.6$ D (*45*), a dielectric constant for the peptide, $\varepsilon_r \approx 5$ (*12*, *46*), and the distance between the side chain and the permeating ion, $r \approx 6.5$ Å. The ion−side chain interaction energy is estimated as $\Delta E = \mu e/(4\pi\varepsilon_0\varepsilon_r r^2)$ or $\sim k_B T$ using the listed parameters, in agreement with the observed conductance changes. As would be expected, apart from the rectification (see below), the effects of the substitutions in the respective subunits are approximately additive (Table 2). It is not clear, however, why the larger current changes are observed for the Ser$^5$ analogues.

*Direction of Current Flow*. For all of the hybrid channels, the single-channel currents in both directions are intermediate between those of the respective homodimeric channels. Furthermore, the currents are always larger when the permeant ions enter the channel's alanine-only subunit and exit from the serine-containing subunit (Figure 6). Moreover, the asymmetry is larger for channels formed by the Ser$^5$ analogues, compared to channels formed by the Ser$^3$ analogues. The latter result can be understood by noting that Ser$^5$ in the $\beta^{6.3}$-helical channel is positioned slightly farther away from the bilayer center than is Ser$^3$. The barrier imposed by the individual Ser side chains therefore appears to be relatively localized, close to the site of the amino acid substitution.

## CONCLUSION

We have taken advantage of the structural framework provided by the bilayer-spanning gA channels to investigate the structural and functional consequences of Ala → Ser substitutions introduced on the lipid-facing channel surface near the bilayer center. The amino acid substitutions do not alter the fold of the conducting channel. The energetic penalty for burying the serine hydroxyl side chain within the bilayer core is ~15 kJ/mol, similar in magnitude to predictions from cyclohexane/water partition coefficients (*41*) and from molecular dynamics simulations (*4*), yet larger than would be predicted from lipid bilayer/water partition coefficients (*44*). The results point toward the importance of knowing the side chain positions within the bilayer when evaluating the functional consequences of polar versus nonpolar substitutions.

## ACKNOWLEDGMENT

We thank Drs. Benoît Roux and Yuhui Li for discussions about serine-containing gramicidin analogues.

## REFERENCES

1. von Heijne, G. (2007) Formation of transmembrane helices in vivo—Is hydrophobicity all that matters? *J. Gen. Physiol. 129*, 353–356.
2. Wolfenden, R. (2007) Experimental measures of amino acid hydrophobicity and the topology of transmembrane and globular proteins. *J. Gen. Physiol. 129*, 357–362.
3. White, S. H. (2007) Membrane protein insertion: the biology-physics nexus. *J. Gen. Physiol. 129*, 363–369.
4. MacCallum, J. L., Bennett, W. F. D., and Tieleman, D. P. (2007) Partitioning of amino acid side chains into lipid bilayers: Results from computer simulations and comparison to experiment. *J. Gen. Physiol. 129*, 371–377.
5. White, S. H., and Wimley, W. C. (1999) Membrane protein folding and stability: Physical principles. *Annu. Rev. Biophys. Biomol. Struct. 28*, 319–365.
6. Engelman, D. M., Steitz, T. A., and Goldman, A. (1986) Identifying non-polar transbilayer helices in amino acid sequences of membrane proteins. *Annu. Rev. Biophys. Biophys. Chem. 15*, 321–353.
7. Dorairaj, S., and Allen, T. W. (2007) On the thermodynamic stability of a charged arginine side chain in a transmembrane helix. *Proc. Natl. Acad. Sci. U.S.A. 104*, 4943–4948.
8. MacCallum, J. L., Bennett, W. F. D., and Tieleman, D. P. (2008) Distribution of amino acids in a lipid bilayer from computer simulations. *Biophys. J. 94*, 3393–3404.
9. Sun, H., Greathouse, D. V., Andersen, O. S., and Koeppe, R. E., II (2008) The preference of tryptophan for membrane interfaces: Insights from N-methylation of tryptophans in gramicidin channels. *J. Biol. Chem. 283*, 22233–22243.
10. Andersen, O. S., Koeppe, R. E., II, and Roux, B. (2005) Gramicidin channels. *IEEE Trans. Nanobiosci. 4*, 10–20.
11. Andersen, O. S., and Koeppe, R. E., II (2007) Bilayer thickness and membrane protein function: An energetic perspective. *Annu. Rev. Biophys. Biomol. Struct. 36*, 107–130.
12. Koeppe, R. E., II, Mazet, J.-L., and Andersen, O. S. (1990) Distinction between dipolar and inductive effects in modulating the conductance of gramicidin channels. *Biochemistry 29*, 512–520.
13. Russell, E. W. B., Weiss, L. B., Navetta, F. I., Koeppe, R. E., II, and Andersen, O. S. (1986) Single-channel studies on linear gramicidins

with altered amino acid side chains. Effects of altering the polarity of the side chain at position 1 in gramicidin A. *Biophys. J. 49*, 673–686.
14. Morrow, J. S., Veatch, W. R., and Stryer, L. (1979) Transmembrane channel activity of gramicidin A analogues: Effects of modification and deletion of the amino-terminal residue. *J. Mol. Biol. 132*, 733–738.
15. Mattice, G. L., Koeppe, R. E., II, Providence, L. L., and Andersen, O. S. (1995) Stabilizing effect of D-alanine-2 in gramicidin channels. *Biochemistry 34*, 6827–6837.
16. Greathouse, D. V., Koeppe, R. E., II, Providence, L. L., Shobana, S., and Andersen, O. S. (1999) Design and characterization of gramicidin channels. *Methods Enzymol. 294*, 525–550.
17. Greathouse, D. V., Hinton, J. F., Kim, K. S., and Koeppe, R. E., II (1994) Gramicidin A/short-chain phospholipid dispersions: Chain length dependence of gramicidin conformation and lipid organization. *Biochemistry 33*, 4291–4299.
18. Weiss, L. B., and Koeppe, R. E., II (1985) Semisynthesis of linear gramicidins using diphenyl phosphorazidate (DPPA). *Int. J. Pept. Protein Res. 26*, 305–310.
19. Andersen, O. S. (1983) Ion movement through gramicidin A channels. Single-channel measurements at very high potentials. *Biophys. J. 41*, 119–133.
20. Sawyer, D. B., Koeppe, R. E., II, and Andersen, O. S. (1989) Induction of conductance heterogeneity in gramicidin channels. *Biochemistry 28*, 6571–6583.
21. Wallace, B. A., Veatch, W. R., and Blout, E. R. (1981) Conformation of gramicidin A in phospholipid vesicles: Circular dichroism studies of effects of ion binding, chemical modification, and lipid structure. *Biochemistry 20*, 5754–5760.
22. Killian, J. A., Prasad, K. U., Hains, D., and Urry, D. W. (1988) The membrane as an environment of minimal interconversion. A circular dichroism study on the solvent dependence of the conformational behavior of gramicidin in diacylphosphatidylcholine model membrane. *Biochemistry 27*, 4848–4855.
23. Mazet, J. L., Andersen, O. S., and Koeppe, R. E., II (1984) Single-channel studies on linear gramicidins with altered amino acid sequences. A comparison of phenylalanine, tryptophan, and tyrosine substitutions at positions 1 and 11. *Biophys. J. 45*, 263–276.
24. Russell, A. J., and Fersht, A. R. (1987) Rational modification of enzyme catalysis by engineering surface charge. *Nature* (*London*) *328*, 496–500.
25. Durkin, J. T., Koeppe, R. E., II, and Andersen, O. S. (1990) Energetics of gramicidin hybrid channel formation as a test for structural equivalence. Side-chain substitutions in the native sequence. *J. Mol. Biol. 211*, 221–234.
26. Becker, M. D., Greathouse, D. V., Koeppe, R. E., II, and Andersen, O. S. (1991) Amino acid sequence modulation of gramicidin channel function: Effects of tryptophan-to-phenylalanine substitutions on the single-channel conductance and duration. *Biochemistry 30*, 8830–8839.
27. Galbraith, T. P., and Wallace, B. A. (1998) Phospholipid chain length alters the equilibrium between pore and channel forms of gramicidin. *Faraday Discuss.,* 159–164 (discussion 225−246).
28. Durkin, J. T., Providence, L. L., Koeppe, R. E., II, and Andersen, O. S. (1993) Energetics of heterodimer formation among gramicidin analogues with an $NH_2$-terminal addition or deletion: Consequences of missing a residue at the join in the channel. *J. Mol. Biol. 231*, 1102–1121.
29. O'Connell, A. M., Koeppe, R. E., II, and Andersen, O. S. (1990) Kinetics of gramicidin channel formation in lipid bilayers: Transmembrane monomer association. *Science 250*, 1256–1259.
30. Sarges, R., and Witkop, B. (1965) Gramicidin A. V. The structure of valine- and isoleucine-gramicidin A. *J. Am. Chem. Soc. 87*, 2011–2020.
31. Hotchkiss, R. D. (1941) The chemical nature of gramicidin and tyrocidine. *J. Biol. Chem. 141*, 171–185.
32. Hotchkiss, R. D. (1944) Gramicidin, tyrocidine, and tyrothricin. *Adv. Enzymol. Relat. Areas Mol. Biol. 4*, 153–199.
33. Koeppe, R. E., II, Paczkowski, J. A., and Whaley, W. L. (1985) Gramicidin K, a new linear channel-forming gramicidin from *Bacillus brevis*. *Biochemistry 24*, 2822–2826.
34. Veatch, W. R., Mathies, R., Eisenberg, M., and Stryer, L. (1975) Simultaneous fluorescence and conductance studies of planar bilayer membranes containing a highly active and fluorescent analog of gramicidin A. *J. Mol. Biol. 99*, 75–92.
35. Veatch, W., and Stryer, L. (1977) The dimeric nature of the gramicidin A transmembrane channel: Conductance and fluorescence energy transfer studies of hybrid channels. *J. Mol. Biol. 113*, 89–102.
36. Cifu, A., Koeppe, R. E., II, and Andersen, O. S. (1992) On the supramolecular structure of gramicidin channels. The elementary conducting unit is a dimer. *Biophys. J. 61*, 189–203.
37. He, K., Ludtke, S. J., Wu, Y., Huang, H. W., Andersen, O. S., Greathouse, D., and Koeppe, R. E., II (1994) Closed state of gramicidin channel detected by X-ray in- plane scattering. *Biophys. Chem. 49*, 83–89.
38. Bamberg, E., and Läuger, P. (1973) Channel formation kinetics of gramicidin A in lipid bilayer membranes. *J. Membr. Biol. 11*, 177–194.
39. Rokitskaya, T. I., Antonenko, Y. N., and Kotova, E. A. (1996) Photodynamic inactivation of gramicidin channels: A flash-photolysis study. *Biochim. Biophys. Acta 1275*, 221–226.
40. Kolb, H. A., and Bamberg, E. (1977) Influence of membrane thickness and ion concentration on the properties of the gramicidin a channel. Autocorrelation, spectral power density, relaxation and single-channel studies. *Biochim. Biophys. Acta 464*, 127–141.
41. Radzicka, A., and Wolfenden, R. (1988) Comparing the polarities of the amino acids: side-chain distribution coefficients between the vapor phase, cyclohexane, 1-octanol, and neutral aqueous solution. *Biochemistry 27*, 1664–1670.
42. Choe, S., Hecht, K. A., and Grabe, M. (2008) A continuum method for determining membrane protein insertion energies and the problem of charged residues. *J. Gen. Physiol. 131*, 563–573.
43. Wimley, W. C., Creamer, T. P., and White, S. H. (1996) Solvation energies of amino acid side chains and backbone in a family of host-guest pentapeptides. *Biochemistry 35*, 5109–5124.
44. Wimley, W. C., and White, S. H. (1996) Experimentally determined hydrophobicity scale for proteins at membrane interfaces. *Nat. Struct. Biol. 3*, 842–848.
45. Smyth, C. P. (1955) Dielectric Behavior and Structure, McGraw-Hill, New York.
46. Tredgold, R. H., and Hole, P. N. (1976) Dielectric behaviour of dry synthetic polypeptides. *Biochim. Biophys. Acta 443*, 137–142.